Supporting Information

Ghazizadeh et al. 10.1073/pnas.1707695115

SI Methods

Subjects. Two adult rhesus monkeys (U: female, D: male) participated in the study. Before training, monkeys were implanted with a head post, which was used to immobilize the head during testing. Both monkeys were also implanted with scleral search coils in one eye. All animal care and experimental procedures were approved by the National Eye Institute Animal Care and Use Committee and complied with the Public Health Service Policy on the humane care and use of laboratory animals.

fMRI Scanning. Functional magnetic resonance images were collected while the monkeys were engaged in a passive viewing task. Structural and functional images were acquired in a 4.7-T, 60-cm vertical scanner (Bruker Biospec) equipped with a Bruker S380 gradient coil. A transmit coil, 20- × 12.5-cm dimensions, was positioned over the posterior portion of the monkey's head. Four circular-shaped receive coil elements, one overlapped pair on each side, were positioned over the temporal-parietal and frontal lobes (diameter 7.2 cm). Subjects sat upright in a specially designed chair and viewed the visual stimuli projected onto a screen above their head through a mirror. Functional echo planar imaging (EPI) scans were collected using a T2* weighted echo-planar sequence [42 sagittal slices, matrix size = 64 × 34, flip angle = 85°, repetition time (TR) = 2.5 s, echo time (TE) = 14 ms, 1.5 mm^3 isotropic voxels]. Fast anatomical scans (T1-weighted MDEFT and gradient echo FLASH, 0.5 × 0.5 × 1.5 mm) were acquired at the end of each session, with slices matching to the functional EPI slices. MION, a T2* contrast agent, was administered before the start of each scanning session. MION doses were determined independently for each subject to attain a consistent drop in the signal intensity of ∼50–60% (81), which corresponded to ∼10 mg/kg MION. Each passive viewing run lasted for 8 min (192 total volumes). Animals could complete multiple runs in a given scanning session. We also collected high-resolution anatomical scans at 0.5-mm isotropic resolution from a horizontal 4.7-T magnet (Bruker Biospec 47/60), while monkeys were under isoflurane anesthesia in an MRI-compatible stereotaxic frame.

Stimuli. We created visual stimuli using fractal geometry (82, 83). One fractal was composed of four point-symmetrical polygons that were overlaid around a common center such that smaller polygons were positioned more toward the front. The parameters that determined each polygon (size, edges, color, etc.) were chosen randomly. Fractal diameters used for value training were on average ∼8°. During scans, fractals were resized to ∼5° to fit the mirror size inside the scanner. Monkeys saw many fractals (U: 104, D: 100 fractals), half associated with large reward (good object) and the other half associated with small reward (bad object) during training.

Stimulus Presentation and Task Control. Value training and free viewing outside the scanner were controlled by custom made C++ based software (Blip, www.robilis.com/blip/). Data acquisition and output control was performed using National Instruments NI-PCIe 6353. Stimuli generated by an active-matrix liquid crystal display projector (PJ550; ViewSonic) were rear-projected on the screen. Eye position was sampled at 1 kHz using a scleral search coil. Inside the scanner, stimuli were rear-projected on a screen above the monkey and reflected through a 45° mirror. Stimulus presentation was done using Psychtoolbox and the event timings and gaze location was controlled and saved by a real-time custom QNX-based program. Eye position was monitored by MR-compatible infrared camera (MRC camera 60 Hz, SMI IView × 2.6, tracking resolution <0.1°).

Stable Value Training. We used an object-directed saccade task to train object–value associations outside the scanner (Fig. 1*A*). Each session of training was performed with a set of eight fractals (four good/four bad fractals). After central fixation on a white dot, one object appeared on the screen at one of the eight peripheral locations (15° eccentricity). After an overlap period of 400 ms, the fixation dot disappeared and the animal was required to make a saccade to the fractal. After 500 ± 100 ms of fixating the fractal, a large (0.3 mL) or small (0.1 mL) reward was delivered. Diluted apple juice (33–66%) was used as reward. The displayed fractal was then turned off followed by an intertrial interval (ITI) of 1–1.5 s with a blank screen. Each training session consisted of 80 trials with each object pseudorandomly presented 10 times. Each object was trained for at least 10 sessions to create stable values. Breaking fixation or a premature saccade to fractal during training resulted in an error tone (<7% of trials). A correct tone was played at the conclusion of a correct trial.

Value Memory: Passive Viewing Task. Neural discrimination of good and bad objects was measured days (1–10 d) or months (6–13 mo) after the last value training session using a passive viewing task in the scanner. Each run consisted of 16 blocks lasting 30 s each (eight base/eight probe). There were four different probe blocks: [good, bad] × [left, right] (Fig. 1*D*). The order of four probe block types was pseudorandomized such that in every four sequential probe blocks all four types were shown and each run consisted of two such randomized cycles. Each block was divided into trials with variable duration (approximately four to five trials per block), which required central fixation on a 0.5° white dot within a 3° × 3° window. During probe blocks, fractals were flashed (600 ms on, 200 ms off) in one hemifield (∼6° eccentricity) in horizontal and 45° oblique directions (pseudorandom location for each object) while the animal maintained central fixation. Three to five consecutive objects were shown during each trial. After the trial, central fixation was extinguished followed by an ITI of 2.2 s during which the animal was rewarded (50–100% apple juice) for fixation. All objects in a given block were chosen from either good or bad categories and were shown on either the right or left visual hemifield. No contingent reward for objects was delivered during passive viewing. Breaking fixation or failing to fixate centrally within 3 s of fixation dot appearance resulted in extinction of all visual stimuli followed by a 2.2 s ITI before start of the next trials. The data analyzed in this study consisted of 19 runs for monkey U and 18 runs for monkey D in day-later scans and 21 runs for monkey U and 14 runs for monkey D in months-later scans.

Value Memory: Free-Viewing Task. Free-viewing sessions were done days (1–10 d) or months (6–13 mo) after training to test behavioral discrimination of good vs. bad objects. Each free-viewing session consisted of 15 trials. In any given trial, four fractals would be randomly chosen from a set of four good and four bad objects. Location and identity of fractals shown in a trial would be chosen at random. Thus, a given trial could have anywhere between zero and four good objects shown in any of the four corners of an imaginary diamond or square around center (15° eccentricities, Fig. 8*B*). Fractals were displayed for 3 s during which the subjects could look at (or ignore) the displayed

fractals. There was no behavioral outcome for free-viewing behavior. After 3 s of viewing, the fractals disappeared. After a delay of 600 ± 100 ms, a white fixation dot appeared in one of nine random locations in the screen (center or eight radial directions). Monkeys were rewarded for fixating that fixation dot. Next display onset with four fractals was preceded by an ITI of ~1.5 s with a blank screen. Monkey U did nine and monkey D did five sessions of free viewing for days-old memories and the same number for months-old memories.

Face-Patch Localizer. A passive viewing task with central fixation was used for face-patch mapping. Each run consisted of 16 blocks lasting 30 s each (eight face/eight object blocks). Stimuli consisted of conspecific monkey faces or ordinary objects that were shown centrally while the monkey fixated a central white dot overlaid on the images. The ordinary objects were chosen from common office objects in the test area or in the animal facility. Animals were familiarized with faces and objects in passive viewing sessions outside the scanner. Other scanning parameters were the same as passive viewing task (monkey U: six runs, monkey D: six runs). In separate scans, familiar neutral fractals that were never associated with reward were used instead of ordinary objects (monkey U: six runs, monkey D: six runs). The results from both types of face-patch localizers were similar and were combined for final analysis.

fMRI Analysis. All fMRI data were analyzed using the AFNI/SUMA software package (AFNI_16.1.06) (84, 85) as well as custom-written MATLAB (MathWorks) programs. Raw images were first converted from Bruker into AFNI file format. Preprocessing order included slice time correction (3dTshift), motion correction (3dvolreg), and correction for static magnetic field inhomogeneities using the PLACE algorithm (86). The resulting EPI images were first aligned to the anatomical FLASH image taken within each session and then they were registered to the FLASH scan from a reference session. Each registered EPI was then despiked, detrended (fourth-order Legendre polynomials), and transformed into percentage change from mean. A high-resolution anatomical scan (0.5 mm isotropic) was also registered to the MDEFT scan from the reference session. The registered high-resolution MDEFT was then transformed (affine + nonlinear 3dQwarp) into a standard atlas space (D99 space) (25). The resulting EPI time series from all runs were concatenated and transformed into the standard space (affine+nonlinear 3dNwarpApply) using the spatial transformation matrix obtained from the high-resolution MDEFT.

The 3D+time series were regressed against the model time series to calculate the beta coefficients that represented the contribution of each factor in percent change from the mean (3dDeconvolve). The model time series consisted of eight regressors ([days, months] × [good, bad] × [right, left hemifield]) that were one during the block satisfying their condition and zero otherwise and were then convolved with a MION hemodynamics. Seventeen nuisance regressors were used including motion and their first derivatives (12 parameters), reward delivery, blinks, and eye position (horizontal, vertical, and interaction). All nuisance time series except the ones related to motion were convolved with MION hemodynamics before regression. A separate regression with one regressor (probe vs. base) and the same nuisance factors was also carried out to find visual beta coefficients for differential response to probe vs. base blocks. These beta coefficients reflected the degree of visual responsivity of voxels and were orthogonal to value-coding and spatial-coding voxels (i.e., switching the value or hemifield labels for a voxel does not change its overall activity). Equal numbers of top visually responsive voxels (highest visual beta coefficients) in each region were then selected to be averaged for comparison of value coding within each region (Figs. 2 and 3). This selection method avoided the selection bias due to value coding and differences in the number of voxels within regions. Since MION results in negative change in the activated regions, the 3D+time series were multiplied by negative one before regression (e.g., Figs. 2–4) or for plotting (Fig. S3). Blocks where subjects refused to fixate or were asleep were excluded from the analysis (<%7 monkey D and <10% in monkey U of all probe blocks and <3% monkey D and <11% monkey U base blocks). Also, the first three TRs in each run were excluded from the regression due to magnetization.

To make whole-brain familywise correction, estimates of spatial smoothness based on the residuals of the regression was obtained using 3dFWHMx and non-Gaussian spatial autocorrelation function (ACF) was obtained (ACF parameters: a = 0.97, b = 1.10, c = 9.01 monkey U and a = 0.98 b = 1.04 c = 7.99 monkey D). Minimum cluster size for two-sided $\alpha < 0.01$ (familywise error) and voxelwise significance of $P < 0.001$ was found using 3dClustSim (10,000 Monte Carlo simulations) to be 4.7 and 4.2 voxels in monkeys U and D, respectively (nearest-neighbor face touching only; NN = 1, same in all clustering analyses in this study). Therefore, in both monkeys, a minimum cluster size of 5 at voxel $P < 0.001$ was used subsequently. Significant clusters were used as a mask to display areas with significant value modulation in days- or months-memory condition (value modulated, Figs. 2–4). Anatomical areas shown in Fig. S4 were annotated using a standard atlas (25).

The whole-brain familywise correction also revealed GB discrimination in four subcortical areas: striatum, amygdala, claustrum, and cerebellum. We further focused in striatum, amygdala, and claustrum as subcortical regions of interests (ROIs) to be further analyzed using small-volume correction. In addition, while we did not observe significant activation in hippocampus using whole-brain correction, given the importance of this structure in some forms of long-term memory this area was also considered as an ROI for more in-depth examination using small-volume correction. ROIs were dilated by two voxels in 0.5-mm high-resolution space before further processing using AFNI 3dROIMaker. Spatial smoothness of noise (3dFWHMx) and Monte Carlo simulations of false-positive clusters (3dClustSim) were repeated by using each of the ROIs as a mask. In both monkeys, minimum cluster size of 2 in amygdala, claustrum, and hippocampus, which corresponded to two-sided $\alpha < 0.01$ at voxel $P < 0.001$ was used. For striatum, minimum cluster sizes of 3 and 2 at voxel $P < 0.001$ corresponding to $\alpha < 0.01$ in monkey U and $\alpha < 0.05$ in monkey D, respectively, were used. For the small-volume correction results shown in Table S2, striatum and claustrum were divided into ventral and dorsal areas using a plane parallel to the CDt and hippocampus in the saggital slices (plane equation: $DV - 0.41 \times AP + 4.68$ in D99 space RAI DICOM coordinates). Voxels above and below this plane were considered dorsal and ventral, respectively. Ventral striatum included CDt and cvPut.

Residuals from the regression were used to calculate the temporal signal-to-noise ratio (tSNR) in each region. In both monkeys tSNR averaged across all cortex was 25 and tSNR averaged within the four subcortical areas shown in Fig. 7 was >28. The minimum detectable effect size (eff) as the function of tSNR was calculated according to (87) $eff = (8/N)^{1/2} erf^{-1}(p)/tSNR{*}MION\_factor$, where N was the number of data points for good vs. bad comparison (only probe block time points counted), erf^{-1} was the inverse complementary error function, and p was the voxel P value. MION_factor was set to 5 to take account of approximately fivefold enhancement of signal compared with BOLD (18). *eff* was calculated at P = 1e-5. Minimum detectable effect size (*eff*) in hippocampus was >0.13% and >0.16% with tSNR 33 and 30 in monkeys U and D, respectively. For comparison, these values were comparable to minimum detectable effect size in striatum, being >0.1% and >0.17% in monkeys U and D, respectively.

The same processing steps and analysis were performed for face localizer scans except that the regression model time series consisted of only two regressors (face and nonface). The same nuisance regressors were used as in value regression. Blocks where subjects refused to fixate or were asleep were excluded from the analysis (<3% monkey D and <5% in monkey U of all face blocks and <10% monkey D and <3% monkey U of all object blocks). Also, the first three TRs in each run were excluded from the regression due to magnetization.

Resting Correlation Analysis. The residuals of the main regression were used for resting correlation analysis (88) (Fig. 6*A*). The average white matter and ventricle time series were regressed out from this residual time series and band passing between 0.01–0.1 Hz was applied (3dBandpass). The first base block period at the beginning of each run was selected and concatenated across all runs (excluding first three TRs for magnetization). The resting-state dissimilarity between all value modulated anatomical areas was calculated as $-\log(|\rho|)$, with ρ being the pairwise Pearson's correlation between the average signal within each ROI. For each anatomical area, only the part that was significantly modulated by days-old or months-old value in at least one monkey was included. This dissimilarity measure will be 0 for fully correlated regions and grows large for uncorrelated signals. Multidimensional scaling on this dissimilarity matrix was used to display resting-state distances in 2D (MATLAB mdscale, Sammon criteria, stress < 0.17, $R^2 > 0.18$, $P < 0.001$ in both monkeys). Clustering of value modulated ROIs based on this resting-state distance was done using density-based clustering [DBSCAN (89)]. Density-based clustering allowed for arbitrary cluster shape and did not require prior knowledge of the number of clusters, unlike more traditional methods such as *k*-means or expectation maximization clustering. The minimum number of points to create a cluster was set to the smallest possible of 2 (i.e., there should be at least two points to be counted as a cluster) and grouping neighborhood was set to be equal to 80th percentile of all pairwise dissimilarities for each monkey (ε = 0.48 monkey U and ε = 0.47 monkey D). This method did not force all points to fall into a cluster and allowed for singleton points (marked with "×" in Fig. 6*B*). Robust linear fits were performed for Fig. 6*C* (MATLAB fitlm, RobustOpts). Correlation coefficient and slopes were obtained after excluding outliers (<9%, bisquare weight <0.5).

For the subcortical functional connectivity with the TP cluster, first the time courses of all areas in the TP clusters were averaged together. Then correlation coefficients (Pearson's) between this average TP cluster signal and all voxels within these four subcortical areas during the first base blocks were obtained. Spatial smoothness of noise (3dFWHMx applied to residuals coming from the TP cluster average used as regressor in 3dDeconvolve) and Monte Carlo simulations of false-positive clusters (3dClustSim) were obtained using small-volume correction by using the four subcortical regions as a mask (ACF parameters: a = 0.98, b = 1.17, c = 10.07, monkey U and a = 0.97, b = 1.05, c = 8.25, monkey D). For subcortical connectivity to the TP cluster, a minimum cluster size of 3 was used for both monkeys, which yielded two-sided $\alpha <$ 0.01 at voxel $P < 0.001$ (ideal values were 3.2 and 2.8 voxels in monkeys U and D, respectively).

Free-Viewing Analysis. Data analysis and statistic tests were done using MATLAB 2016b using custom-written software. Gaze locations were analyzed in an automated fashion and saccades (displacements >2.5°) vs. stationary periods were separated in a given trial (21). Objects were considered to be fixated when gaze was within a 6° window of their center with a stationary period present. Behavioral discrimination of good vs. bad objects was quantified using the area under the receiver operating curve (AUC). AUC was calculated in each session (Fig. S11) and then averaged across sessions for each monkey (Fig. 8).

Fixational Saccade Analysis. Data analysis was done using MATLAB 2016b using custom-written software. Small saccades (0.2–2.5° displacements) during fixation in the scanner were counted as fixational saccades. They were binned across eight diagonal directions and normalized by occurrence in time (hertz) in good and bad blocks. Data from left and right hemifield were averaged such that direction zero was in the presentation hemifield (Fig. S1*B*).

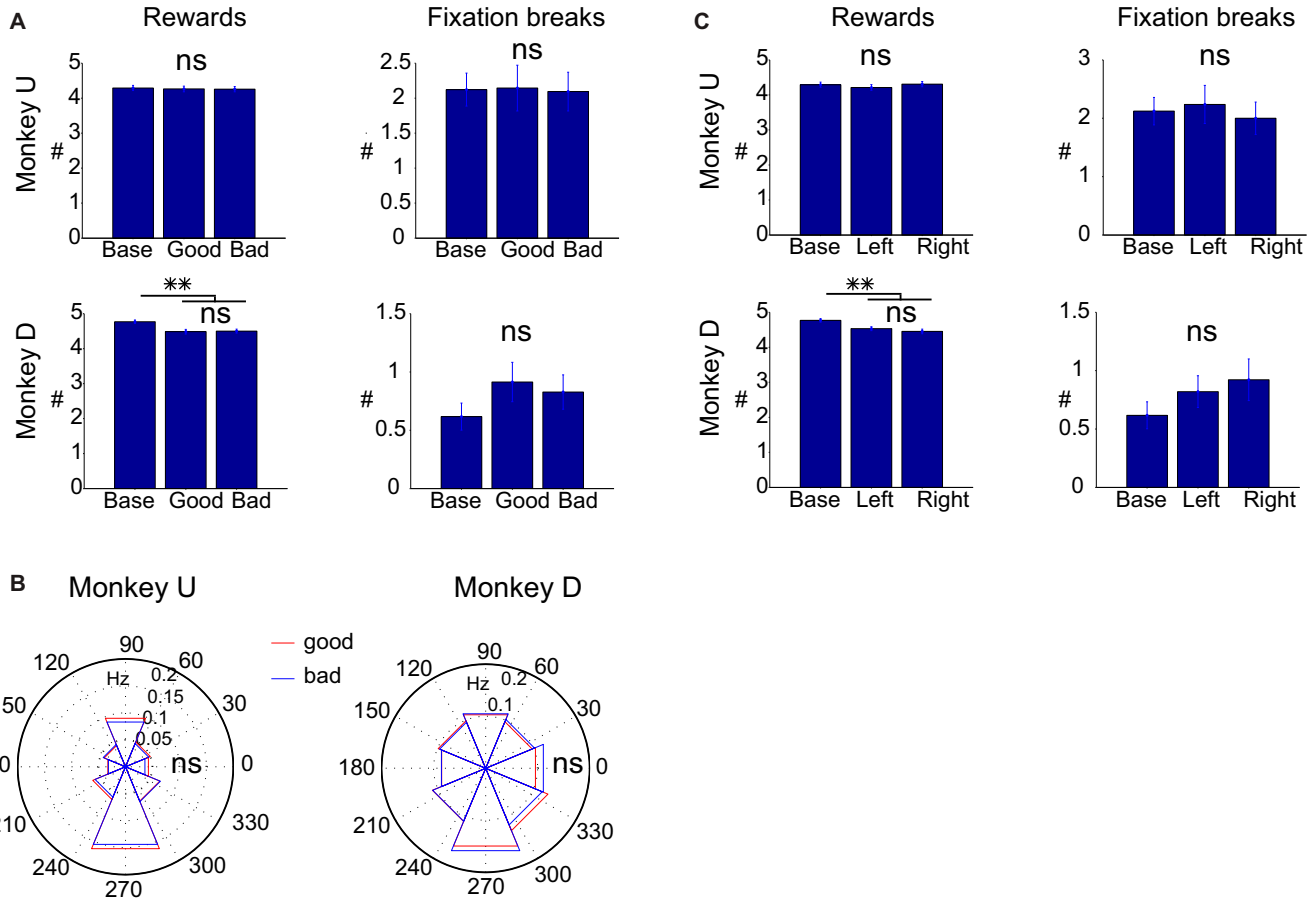

Fig. S1. Equivalent reward and performance across blocks during fMRI. Related to Fig. 1. (*A*) Number of rewards delivered (*Left*) and fixation breaks (*Right*) in the base, good, and bad presentation blocks. Main effect of total rewards received was $F(2, 637) = 0.05$, $P > 0.9$ in monkey U and $F(2, 509) = 9.04$, $P < 1e\text{-}3$ in monkey D. Post hoc test in monkey D showed significant difference between base vs. good or bad blocks ($P < 0.01$) and no significant difference between good and bad ($P > 0.9$). Main effect of total fixation breaks was $F(2, 637) = 0.006$, $P > 0.9$ in monkey U and $F(2, 509) = 1.3$, $P = 0.26$ in monkey D [ns, not significant, $^{**}P < 0.01$ post hoc honest significant difference (HSD)]. (*B*) Frequency (hertz) of fixational saccades (0.2–2.5° saccade size) in the eight radial directions in good and bad blocks. Saccade directions were reflected such that 0° and ± 45° directions were in the object presentation hemifield. Main effect of good vs. bad and interaction with the eight directions were $F(1, 624) = 1.4$ and $F(7, 624) = 0.22$ in monkey U, respectively, and were $F(1, 496) = 0.38$ and $F(7, 496) = 0.49$ in monkey D, respectively, with $P > 0.2$ in all cases (ns, not significant). (*C*) Same format as *A* but for the base, left, and right presentation blocks. Main effect of total rewards received was $F(2, 637) = 0.31$, $P > 0.7$ in monkey U and $F(2, 509) = 9.4$, $P < 1e\text{-}4$ in monkey D. Post hoc test in monkey D showed significant difference between base vs. good or bad blocks ($P < 0.01$) and no significant difference between good and bad ($P > 0.6$). Main effect of total fixation breaks was $F(2, 637) = 0.14$, $P > 0.8$ in monkey U and $F(2, 509) = 1.3$, $P = 0.26$ in monkey D. (ns, not significant, $^{**}P < 0.01$ post hoc HSD).

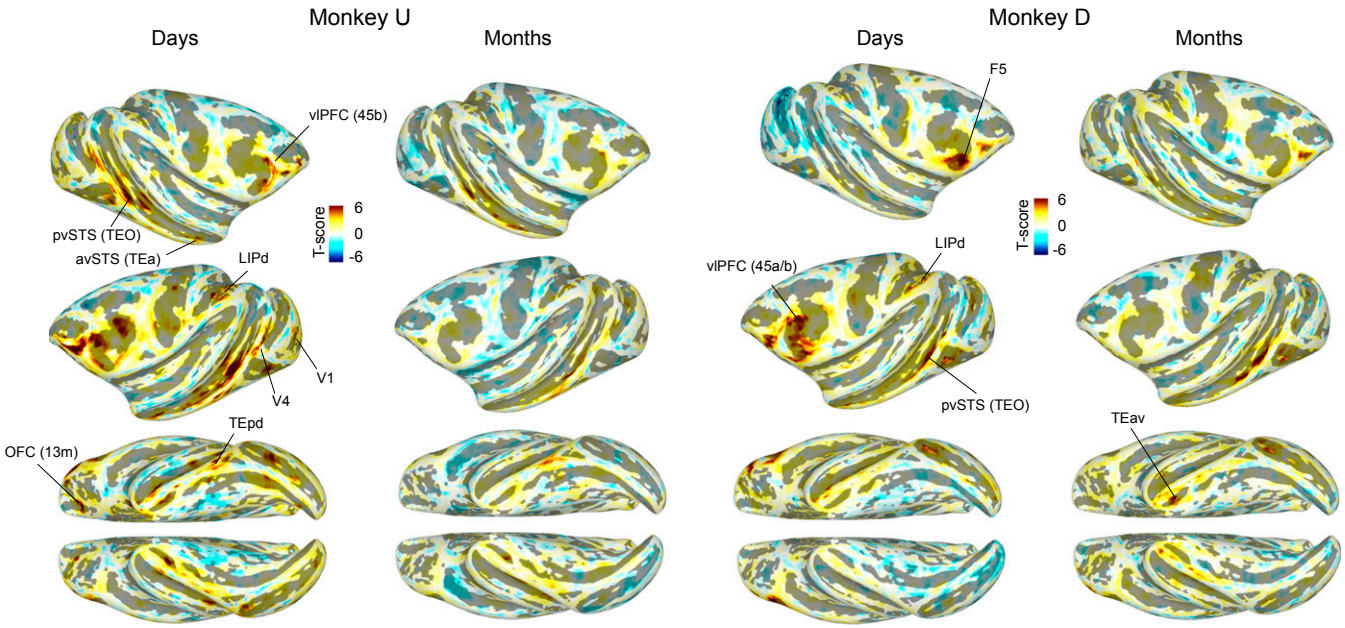

Fig. S2. GB discrimination by days-old and months-old values: T scores. Related to Figs. 2–4. Unthresholded T scores for good–bad contrast in days-later and months-later scans in both hemispheres and on the ventral surface for both monkeys. Regions with higher saturation are more significantly modulated by days- or months-old values. Warmer colors mean bigger activation to good compared with bad and cooler colors mean the opposite. Some areas with strong value modulation in temporal, prefrontal, and parietal area are annotated (LIPd, dorsal lateral intraparietal area).

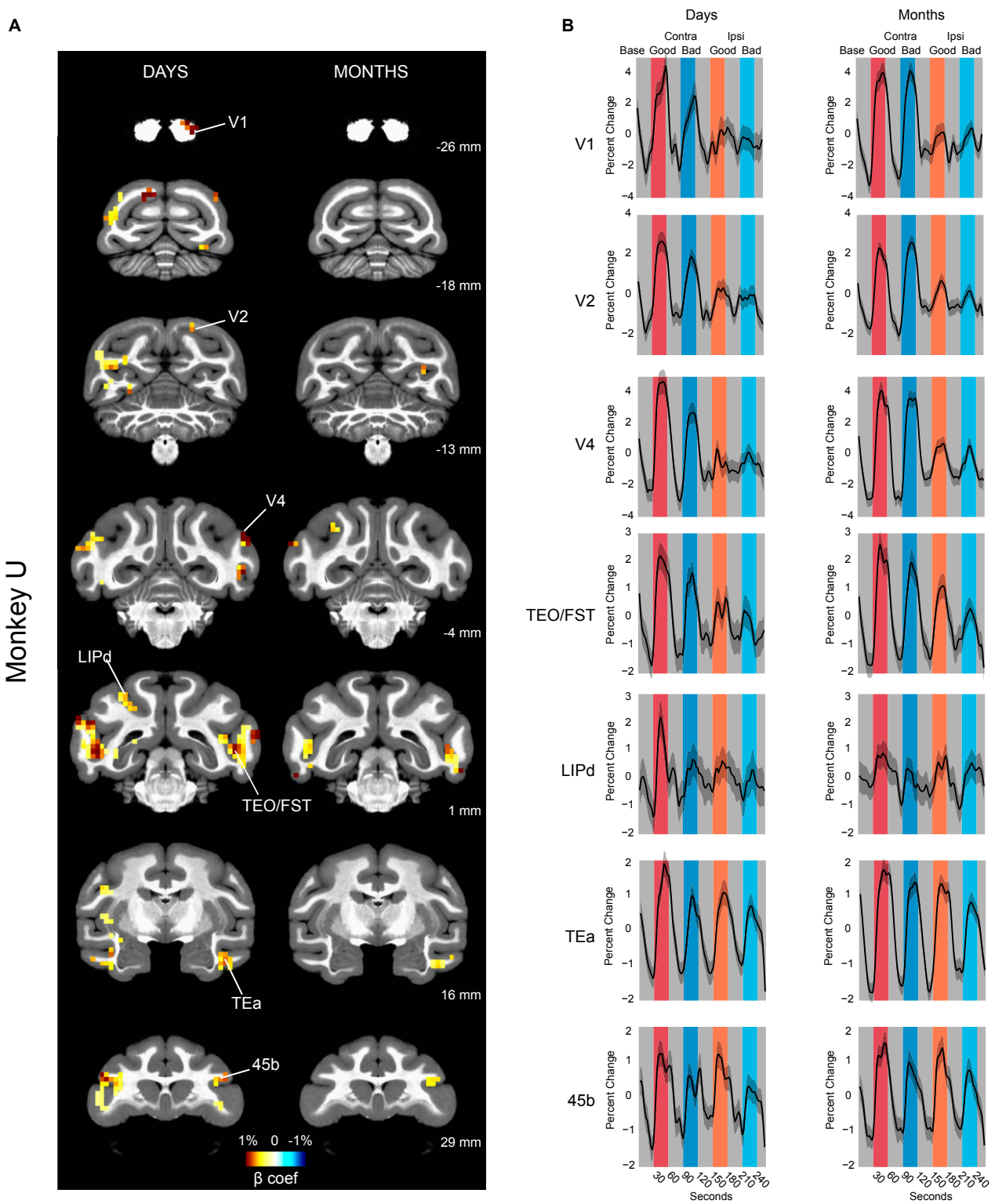

Fig. S3. GB discrimination and activation time courses in days- and months-later scans in example voxels. Related to Figs. 2 and 3. (*A*) Example coronal sections from posterior to anterior (distance to interaural shown): voxels with significant GB discrimination are shown for days-later (*Left*) and months-later scans (*Right*) with color-coded beta coefficients for good–bad contrast ($P < 0.001$, $\alpha < 0.01$ cluster-corrected). (*B*) Concatenated fMRI average time course for the voxels marked in *A* across base and four different probe blocks (color-coded as in Fig. 1*D*) in days-later (*Left*) and months-later (*Right*) scans. The shading shows the SEM. Time courses are multiplied by −1 to account for use of MION. Data in this figure are from monkey U.

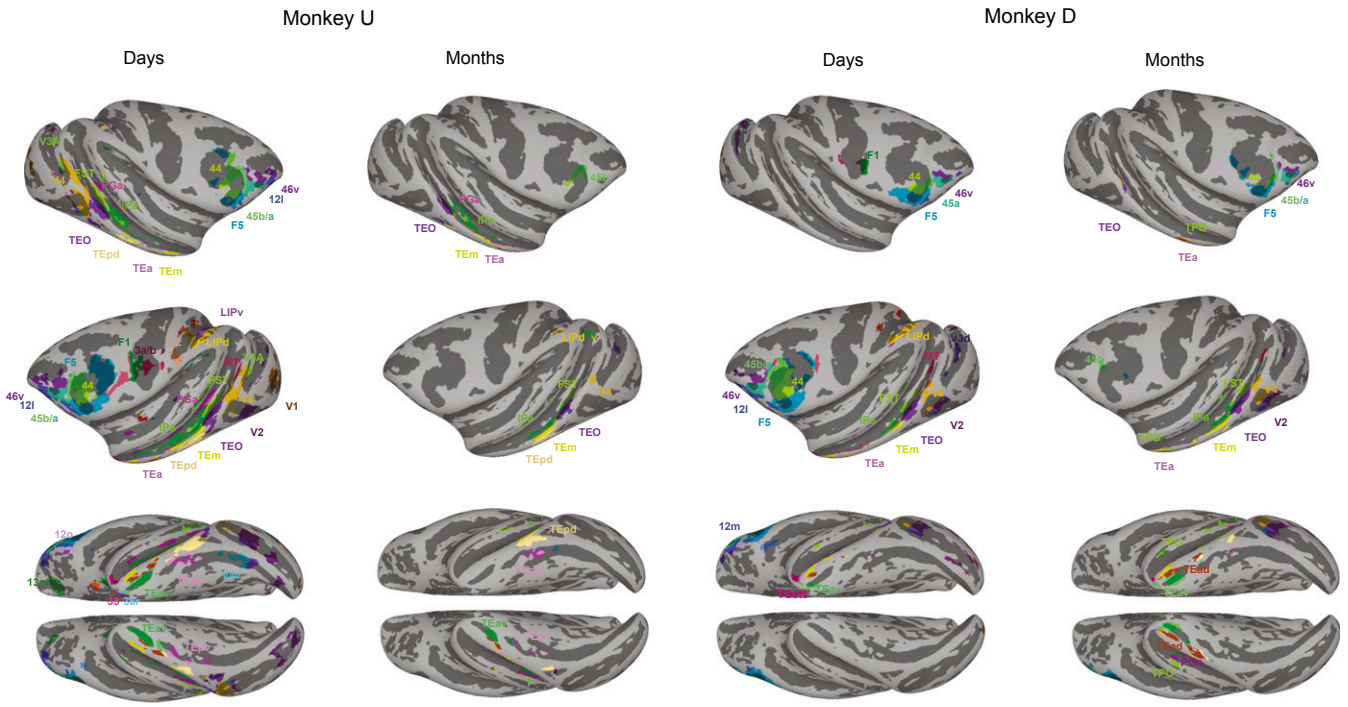

Fig. S4. Anatomical areas with significant GB discrimination in days-later or months-later scans. Related to Fig. 4. Areas with significant GB discrimination in Fig. 4 are used as a mask on the Saleem and Logothetis atlas (90) to find the anatomical cortical areas involved in long-term value memory (to see all 60 anatomical areas found see Table S1). Some of the areas are annotated. For the correspondence of all colors to areas refer to ref. 25.

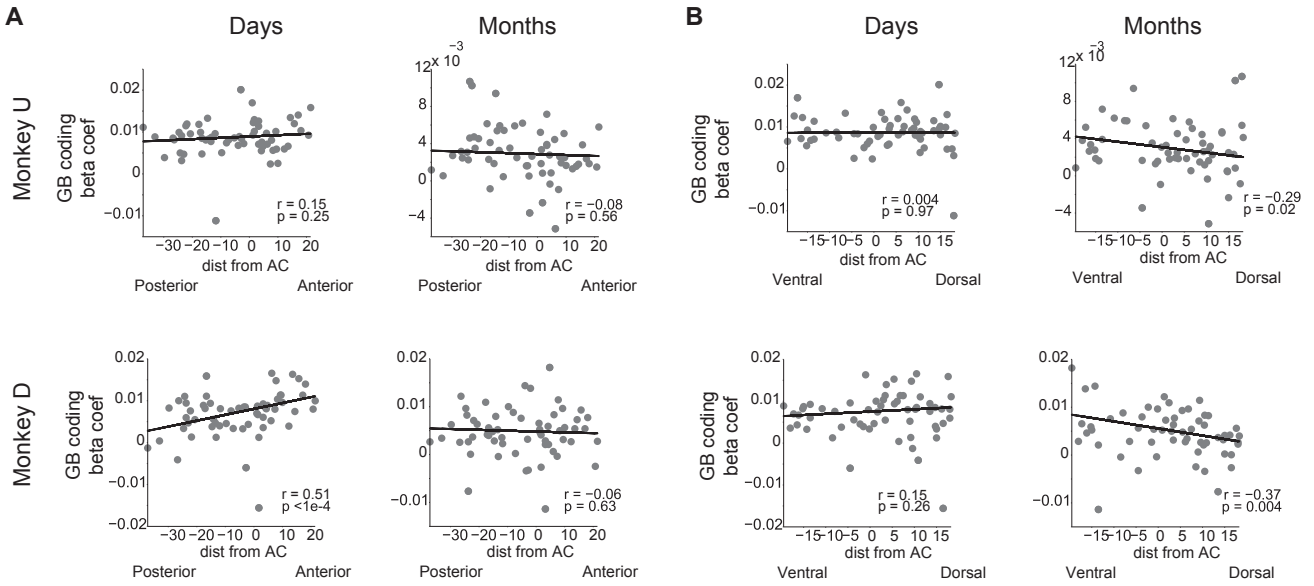

Fig. S5. Strength of GB coding as a function of anterior–posterior and ventral–dorsal position of value-coding areas. Related to Fig. 5. (*A*) Beta coefficients ($n = 60$) for days- and months-old value as a function of anterior–posterior distance from anterior commissure (AC). (Pearson's correlation "*r*" and significance "p" are noted in each plot). (*B*) Same as *A* but for dorsoventral distance from AC.

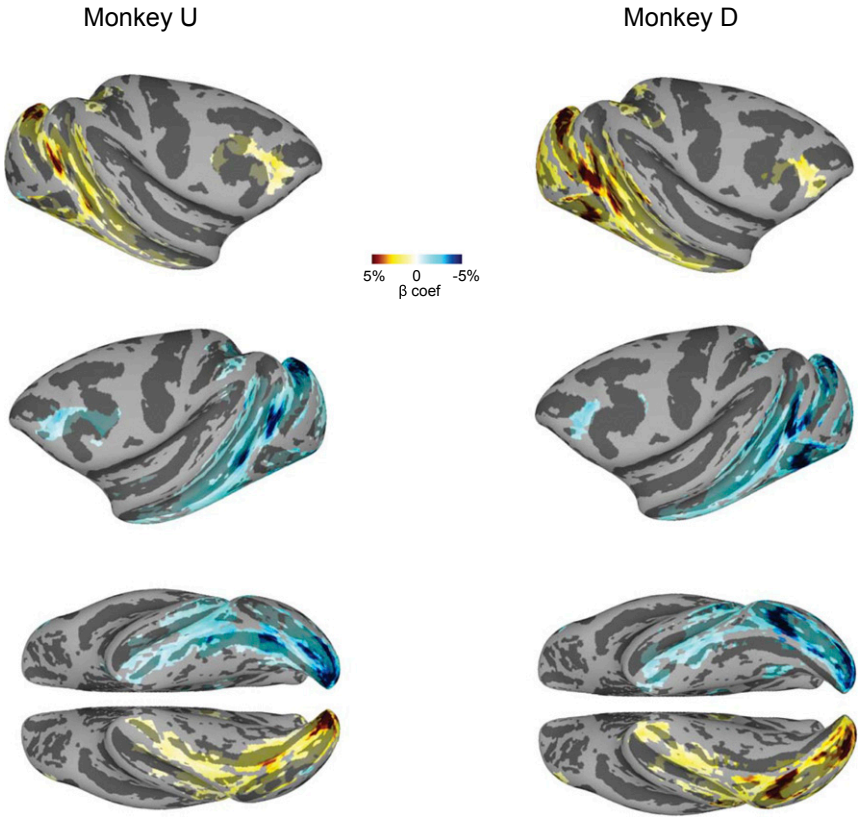

Fig. S6. Areas with significant hemifield selectivity. Related to Fig. 5. Spatial beta coefficients for areas with significant hemifield discrimination in both hemispheres and on the ventral surface for both monkeys ($P < 0.001$, $\alpha < 0.01$ cluster-corrected). Higher saturation means stronger hemifield selectivity. Warm colors mean left > right hemifield selectivity and cool colors mean the opposite.

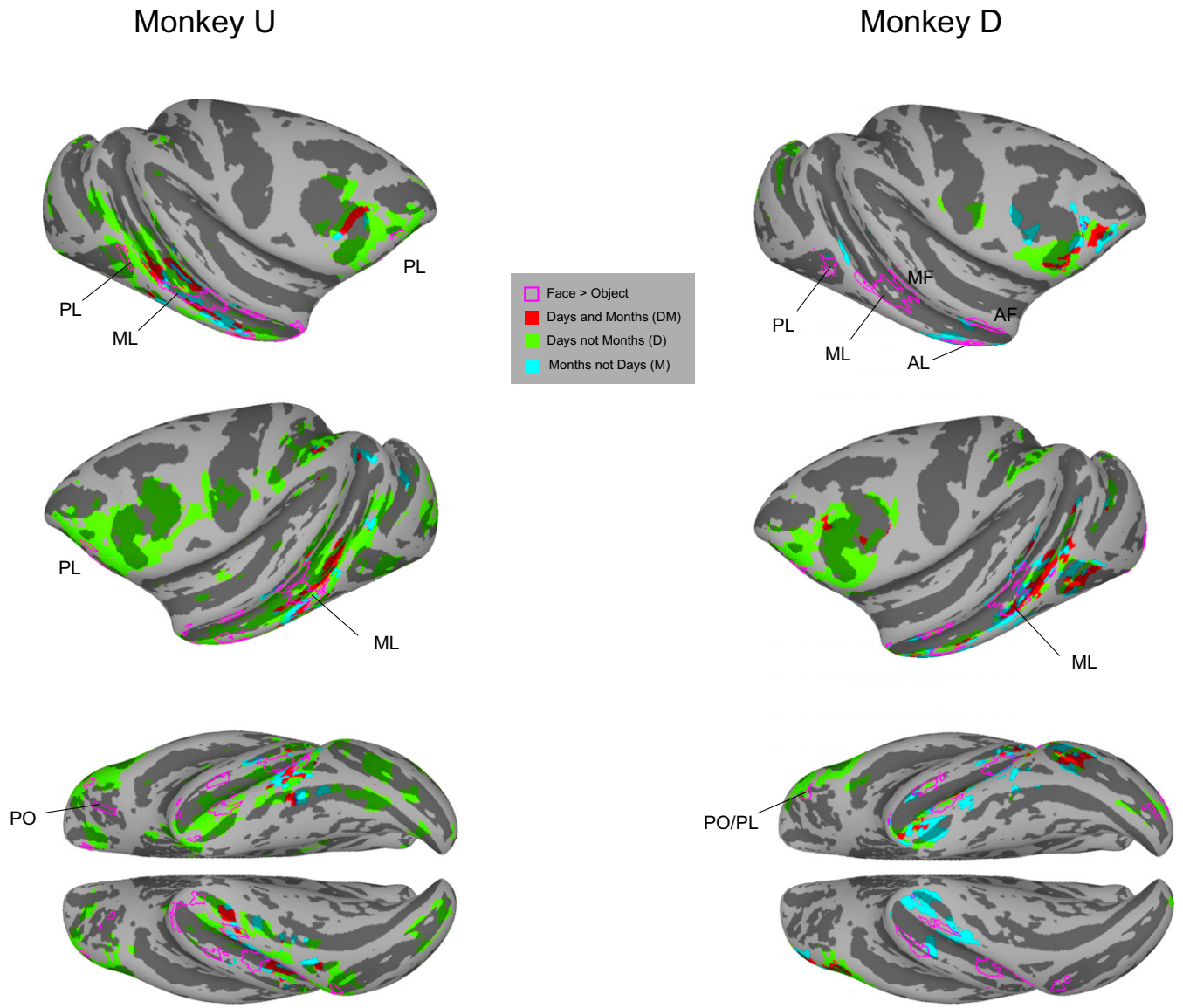

Fig. S7. Relationship between value-coding areas and face patches. Related to Fig. 5. Areas with GB discrimination in days and in months (D, M, and DM voxels) are shown together with face selective areas (face > nonface, pink contour). Temporal and prefrontal face selective areas are annotated.

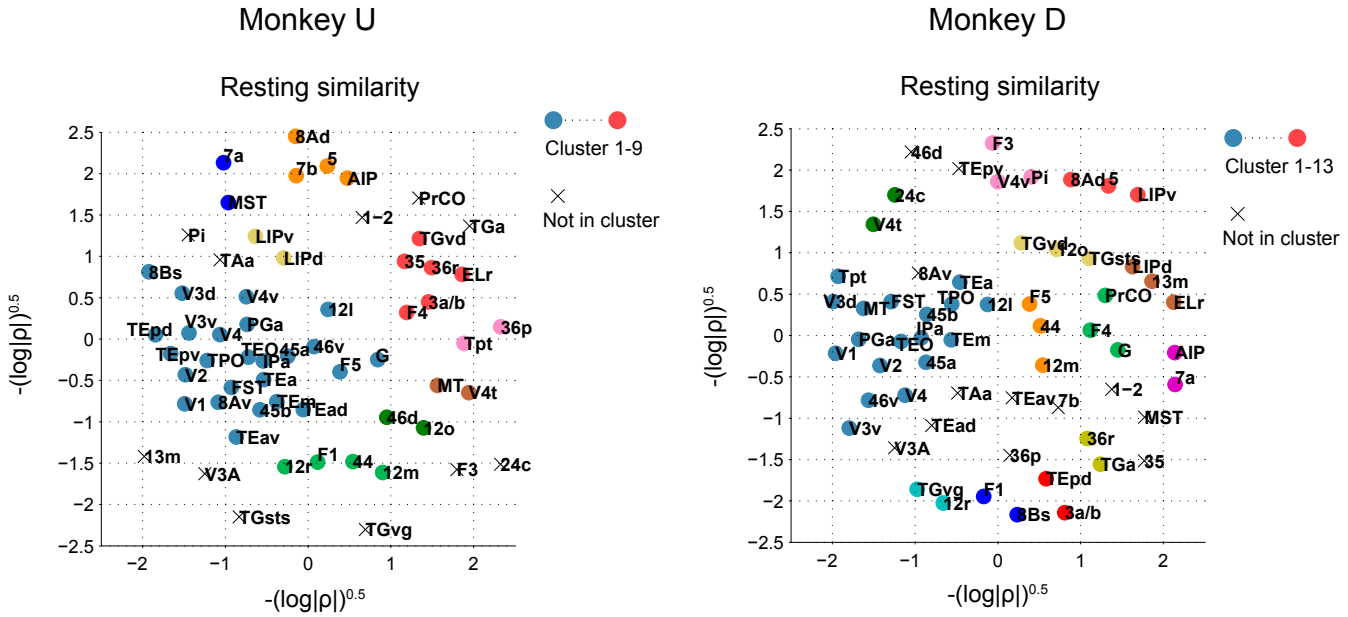

Fig. S8. Resting-state similarity across all value-coding areas displayed in 2D space using multidimensional scaling and colored by density-based clustering. Related to Fig. 6. Same data as Fig. 6*B* but showing the anatomical names of all of the regions with significant days- or months-old GB coding in either monkey. For naming convention see Saleem and Logothetis (90).

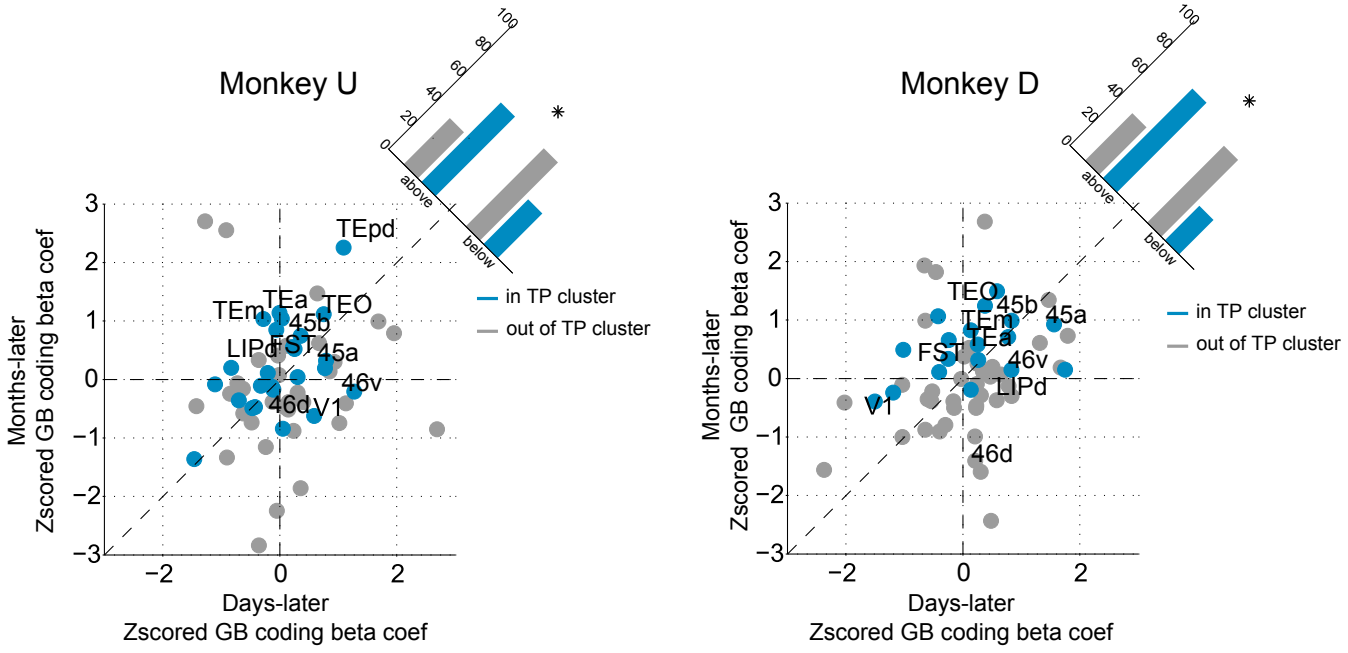

Fig. S9. Regions in TP cluster tend to have stronger GB discrimination after months compared with regions out of TP cluster. Related to Fig. 6. Plots show the *Z*-scored beta coefficients [i.e., [β − avg(β)]/std(β) across value-coding regions] for months- vs. days-old values across value-coding regions to allow comparison with the unity line. A significantly higher percentage of areas in compared with out of TP cluster regions were above the unity line ($\chi^2 > 4.2$, $P < 0.05$ both monkeys). Regions in vlPFC (45a/b and 46) and area TEO were found in the top-right quadrant, consistent with their stronger GB coding compared with other value-coding areas in both days- and months-later scans.

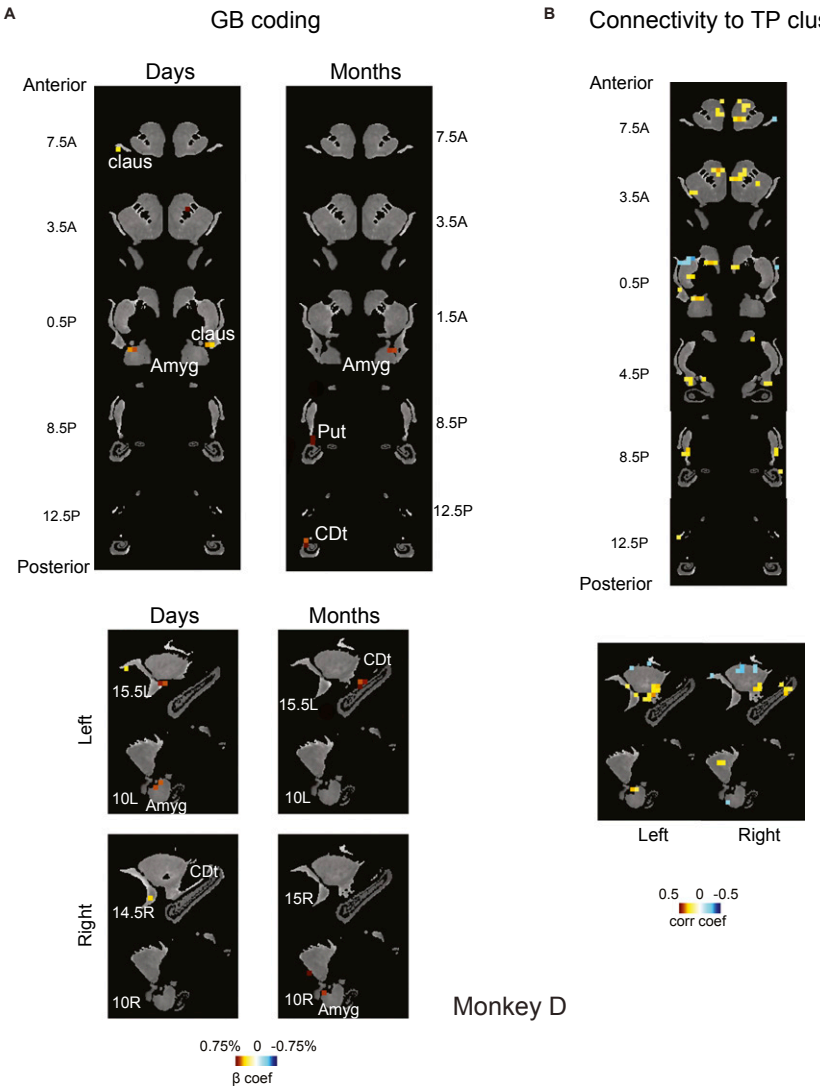

Fig. S10. GB discrimination in striatum, amygdala, claustrum, and hippocampus. Related to Fig. 7. (*A* and *B*) Same format as Fig. 7 but for monkey D.

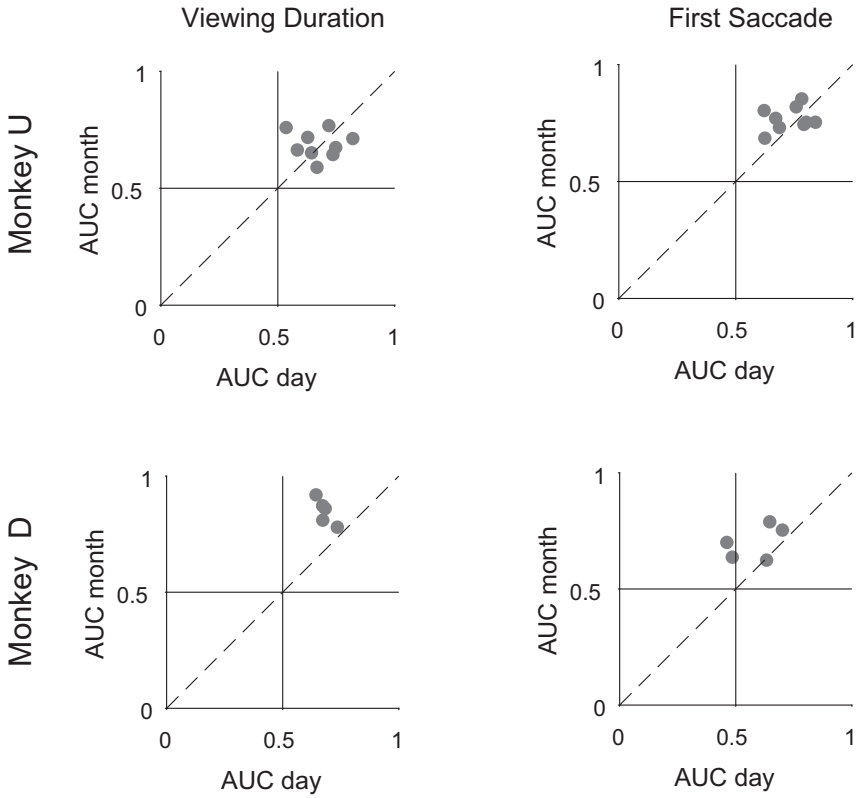

Fig. S11. Behavioral GB discrimination shown separately for each set tested in months- vs. days-later free viewing. Related to Fig. 8. Behavioral discriminability (AUC) of objects for the same set of objects tested in months- vs. in days-later free-viewing sessions as measured by viewing duration or first saccade after display onset.

Table S1. List of all cortical regions [standard atlas Saleem and Logothetis (90)] with D, M, or DM voxels in both monkeys

Region	Area	Monkey U	Monkey D
Frontal lobe	12r	D	D M
	12m	D	D
	13m	D	—
	12l	D	D
	12o	D	D
	PrCO	—	D
	46d	D	D
	46v	D	D M DM
	45a	D	D M DM
	44	D	D M
	45b	D M DM	D M DM
	8Av	D	D M DM
	8Ad	—	D
	8Bs	D	D
	F5 (6Va/6Vb)	D	D M DM
	G	D	D
	F4	D	D
	F3	D	—
	F1 (4)	D	D
Parietal lobe	3a/b	D	D
	1–2	D	—
	7b (PFG/PF)	—	D
	AIP	D	—
	5 (PEa)	D	D
	LIPd	D DM	D
	LIPv	D M	D
	7a (Opt/PG)	M	—
Temporal lobe	TGvg	—	M
	TGsts	D	D DM
	TGvd	D	—
	36p	D	—
	TGa	D	—
	24c	D	—
	35	D	—
	ELr	D	—
	36r	D	—
	TEav	D M DM	D M DM
	Pi	D	–
	TEad	D DM	D M DM
	TEa	D M DM	D M DM
	TEm	D M	D M DM
	TPO	D M DM	D M DM
	TEpv	D M DM	—
	PGa	D M DM	M
	IPa	D M DM	D M DM
	TEpd	D M DM	M
	TAa	D M	—
	TEO	D M DM	D M DM
	FST	D DM	D M DM
	Tpt	D	—
	MST	M DM	–
	MT	D	D M DM
Occipital lobe	V4	D M DM	D M DM
	V4t	D	—
	V4v	D M	DM
	V3v	D	D M DM
	V3A	D	—
	V3d	D M	D M DM
	V2	D M	D M DM
	V1	D M	D

Significant voxels determined at voxel $P < 0.001$ and cluster-corrected for the whole brain at $\alpha < 0.01$.

Table S2. List of subcortical regions [standard atlas Saleem and Logothetis (90)] with D, M, or DM voxels in both monkeys

Area	Monkey U	Monkey D
vPut & CDt	D M DM	M
v-Claustrum	D DM	D M
d-Striatum	D M	D
d-Claustrum	D	D
Amygdala	D M DM	D M
Hippocampus	D	—

Significant voxels determined at voxel $P < 0.001$ and cluster-corrected within four ROIs (striatum, amygdala, claustrum, and hippocampus) using small-volume correction at $\alpha < 0.01$. The D voxel in hippocampus of monkey U belonged to its most posterior region at 16, 21, 0.5 RAI DICOM standard atlas. v- and d-Claustrum, ventral and dorsal claustrum, respectively; d-Striatum, dorsal striatum, which included all striatum but not cvPut and CDt.